Astrocytes grown in Alvetex® 3 dimensional scaffolds retain a non-reactive phenotype

Christopher I Ugbode[1,2], Warren D. Hirst[3], Marcus Rattray[1,4]

[1]School of Pharmacy, Faculty of Life Sciences, University of Bradford, Richmond Road, Bradford, BD7 1DP, UK

[2]Reading School of Pharmacy, University of Reading, Whiteknights, Reading RG6 6UB, UK

[3]Neurodegeneration and Neurologic Diseases, Pfizer Neuroscience Research Unit, 700 Main Street, Kendall Square, Cambridge, Massachusetts, 02149, USA.

Running Title: astrocyte phenotype in 3D Alvetex scaffold

[4]To whom correspondence should be addressed: (email m.rattray@bradford.ac.uk)

Abstract

Protocols which permit the extraction of primary astrocytes from either embryonic or postnatal mice are well established however astrocytes in culture are different to those in the mature CNS. Three dimensional (3D) cultures, using a variety of scaffolds may enable better phenotypic properties to be developed in culture. We present data from embryonic (E15) and postnatal (P4) murine primary cortical astrocytes grown on coated coverslips or a 3D polystyrene scaffold, Alvetex. Growth of both embryonic and postnatal primary astrocytes in the 3D scaffold changed astrocyte morphology to a mature, protoplasmic phenotype. Embryonic-derived astrocytes in 3D expressed markers of mature astrocytes, namely the glutamate transporter GLT-1 with low levels of the chondroitin sulphate proteoglycans, NG2 and SMC3. Embroynic astrocytes derived in 3D show lower levels of markers of reactive astrocytes, namely GFAP and mRNA levels of LCN2, PTX3, Serpina3n and Cx43. Postnatal-derived astrocytes show few protein changes between 2D and 3D conditions. Our data shows that Alvetex is a suitable scaffold for growth of astrocytes, and with appropriate choice of cells allows the maintenance of astrocytes with the properties of mature cells and a non-reactive phenotype.

Key words: glia, EAAT2, scaffold, astrogliosis, cell culture, GLT-1, GFAP.

Introduction

Astrocytes are important cells of the central nervous system (CNS) with a wide range of properties [1-3]. Functions ascribed to astrocytes include supplying neurons with lactate, uptake and conversion of L-glutamate to glutamine [4-7], and secretion of glutathione in response to the generation of reactive oxygen species [8]. They control the composition of the extracellular microenvironment [9], and regulate blood flow through control of local vasculature [10]. Astrocytes also influence synaptic function through potassium uptake, mainly though Kir 4.1 [11] and glutamate uptake [12]. Astrocytes change their phenotype in response to CNS injury in an incompletely-understood process called reactive astrogliosis. Reactive astrogliosis *in vivo*, encompasses a variety of phenotypical and morphological changes in astrocytes which occur over time and differ dependent on the type of injury [13]. The main hallmark of gliosis is an increase in levels of the intermediate filament protein, glial fibrillary acidic protein (GFAP), a protein almost exclusively enriched in astrocytes [14] which appears as a thickening of intermediate filaments, allowing reactive astrocytes to be distinguished from quiescent astrocytes in tissue sections [15, 16]. Reactive astrocytes can protect or exacerbate ongoing neuronal pathology [17-20]. In some human neurodegenerative diseases and animal models of disease, reactive astrocytes with elevated GFAP show a loss of the abundant excitatory amino acid transporter 2 (EAAT2, also known as GLT-1 in rodent species) [21, 22]. Transcriptomic analysis in different pathological models show that astrocytes have distinct gene expression profiles under different types of CNS insult [13] with a range of proteins beyond GFAP and EAAT2 that are regulated.

Whilst *in vivo* research shows consistent data regarding astrocyte phenotype in different pathological models, progress is limited by cell models. *In vitro* models yield astrocytes which are partially representative of cells in the adult brain [23, 24]. Such preparations

yield astrocytes lacking their key transport and metabolic proteins and their characteristic protoplasmic morphology [23]. Mechanical (trituration) or chemical (trypsin) based dissociation also yields astrocytes which express very high levels of GFAP [25]. In addition, pure astrocyte cultures lack the neuronal interactions which regulate phenotype of astrocytes in vivo, for example culture of astrocytes without neurones causes reduction in expression of EAAT-2/GLT-1 [22].

There have been recent developments in creating new in vitro models to study the function of astrocytes. Scaffolds have been used to recreate aspects of the 3 dimensional arrangement of astrocytes in vitro, for example using collagen [26, 27], hydrogels [12, 28], tripalmitin [29] and poly-ε-caprolactone electrospun scaffolds [28, 30, 31]. In this study, we report the use of Alvetex, a commercially available porous scaffold formed of polystyrene that is supplied as cell culture inserts of 200µm thickness [32]. Here we report some of the phenotypic features of astrocytes grown in this way compared to conventional two-dimensional (2D) cultures. We compared astrocytes cultured using two different techniques: cultured from embryonic mice, using a method that was developed in this lab that preserves the adult astrocyte marker EAAT2/GLT-1 expression on cultured astrocytes [21], and the more commonly used method to culture astrocytes from postnatal brains and re-plate [22, 33, 34].

Experimental Procedures

Animal Groups and cell preparation

Timed mated female NIH Swiss mice and P4 NIH Swiss neonates (Harlan UK) were euthanized in accordance with the UK Animals (Scientific Procedures) Act (1986). Animals were killed using cervical dislocation, according to Home Office guidelines. Cerebral cortices from E15 mouse embryos (embryonic) or P4 pups (postnatal) were obtained and cells were isolated via mechanical dissociation as previously described [35]. The cell suspension was centrifuged (5 min, 200g) and re-suspended in the appropriate media (see below).

For embryonic astrocyte cultures, cells were plated in astrocyte specific media (DMEM/F-12 (HAM) GIBCO® Astrocyte Medium – Life Technologies) supplemented with glucose (33mM), L-Glutamine (2mM), 10% FBS and sodium bicarbonate (13mM) (all other reagents obtained from Life Technologies).

For postnatal (P4) astrocyte cultures, the cerebral cortices were dissected and triturated in 1 x HBSS containing L-glutamate (2mM), penicillin (100units/mL) and streptomycin (0.1 mg/mL) (all reagents obtained from Life Technologies). The supernatant was removed and tissues were mixed with 2ml Earle's balanced salt solution (EBSS – Containing 20 units/ml Papain and 0.5mM EDTA (Sigma)), 10µl of DNAse 1 (20,000 Units, Life Technologies) and incubated at 37°C for 15 minutes. The mixture was further triturated with MEM complete medium containing L-Glutamine (2mM), FBS (10%), penicillin (100units/mL) and streptomycin (0.1 mg/mL) supplemented with bovine serum albumin (BSA, Sigma) and trypsin inhibitor (ovomucoid - 1mg/ml respectively, Sigma). The remaining cell suspension was mixed with 5ml of MEM (without BSA and ovomucoid), centrifuged at 1500RPM for 7 minutes and the resulting pellet plated in

DMEM containing L-Glutamine (2mM), FBS (10%), penicillin (100units/mL) and streptomycin (0.1 mg/mL) into 175 cm^2 flasks pre-coated with poly-D-lysine (0.1mg/ml, Sigma) allowing 2 cortices per flask. Cells were cultured for 18-21 days after which microglia were shaken off in an orbital shaker (200 RPM for 5 hours) and the remaining astrocytes were washed with PBS (37°C) and trypsinsed using 0.25% trypsin-EDTA for 5 minutes (Life technologies) and seeded into 6 or 12 well plates. After a further 3 *DIV*, cells were harvested for experimental use.

Two-dimensional Cell Culture system

13mm glass coverslips (0.13mm thick, VWR International Ltd, Lutterworth, UK) were coated with poly-L ornithine (1.5µg/mL solution, Sigma, Dorset, UK) for 24 hours. Afterwards, coverslips were washed with sterile phosphate buffered saline (PBS, , Life Technologies, Paisley, UK) supplemented with glucose (33mM), penicillin (100units/mL) and streptomycin (0.1 mg/mL) (reagents from Life Technologies), and incubated in serum containing medium (10% foetal bovine serum (FBS), Labtech, Uckfield, UK) for 2 hours 37°C and 5% CO_2 before plating. Embryonic or postnatal cells were plated at density of 8 x 10^5 cells/mL into 6 well plates or 4 x 10^5 cells/mL onto coverslips in 12 well plates and maintained for 10-12 d (embryonic) or 3d (postnatal) in the appropriate growth media.. After 10-12 days *in vitro* (DIV), 2D primary cortical astrocyte controls were 90-100% confluent.

Three-dimensional cell Culture system

In order to grow cells in three-dimensions (3D), we used a 200µm thick polystyrene scaffold: Alvetex® (Reinnervate, Durham, UK). We used both 6 well (AVP004-3, 22mm diameter, Reinnervate) and 12 well (AVP005-3, 15mm diameter, Reinnervate) in-well inserts to grow cells in 3D. To render the scaffold hydrophilic, inserts were first fully

submerged in 70% ethanol for 10 minutes. The inserts were then washed twice with sterile water and then incubated with poly-L-ornithine (1.5µg/ml) for 24 hours. After coating, the inserts were washed with PBS and finally incubated in serum containing media for two hours at 37°C and 5% CO_2 before plating cells.

Embryonic or postnatal cells were plated on pre-coated Alvetex (Reinnervate, Durham, UK, see below for details of pretreatment) either into 6 well plates containing Alvetex® inserts at a density of $8x10^5$ cells per mL or into 12 well plates containing Alvetex® inserts at a density of at 4 $x10^5$ cells/mL. Inserts were seeded by applying the cell suspension to the top of the membrane.

Immunofluorescence and cell characterisation

To characterize cell morphology, cells on coverslips and in Alvetex were fixed using 4% paraformaldehyde (PFA; 30 min at room temperature, Sigma) dissolved in PBS; blocked and permeabilised in 1% normal goat serum (NGS, Labtech) and 0.2% Triton-X (Sigma) in PBS, for 1 hour at room temperature (22°C). For GFAP fluorescence, cells were incubated with a mouse polyclonal GFAP primary antibody (Dako, Ely, UK. 1 in 2000) in PBS containing 1% NGS (PBS/NGS) overnight (~18hrs) at 4°C. Cells were further incubated with a secondary antibody conjugated to Alexafluor 488 (in PBS/NGS, 2µg/ml - Invitrogen; Life Technologies), for 90 minutes at room temperature (22°C). After 90 minutes, cells were washed and incubated with Hoescht 33342 (4µg/ml – 5 minutes; Life Technologies) and mounted on microscope slides using Vectashield (Vector Laboratories, Peterborough, UK).

Images were collected on an inverted spinning disc confocal (Zeiss Axiovert 200M) microscope connected to an LSM 510 laser scanning module (Zeiss) and diode (Coherent). 10x/20x and 40x Plan-NeoFluar objectives were used and images were

collected using a colour camera (Zeiss AxioCam HRc colour camera) and processed using Volocity software. High resolution images were created using Photoshop CS3.

Proliferation and MTT Turnover

E15 and P4 astrocytes were seeded into 12 well plates onto treated plastic or Alvetex scaffold. We monitored MTT turnover as previously described [35]. In short, cells were washed with HBM buffer (4.76 g HEPES, 40.88 g NaCl, 0.372 g KCl, 0.42 g $NaHCO_3$, 0.1654 g NaH_2PO_4, 0.3 g Glucose and 240 µl of 0.5 M $CaCl_2$ (Sigma)) and further incubated with 500µl of MTT buffer per well (0.5 mg/ml Thiazoyl Blue Tetrazolium Bromide (Sigma) in HBM) at 37°C for 1 h. The formazide precipitate (MTT) was then solubilised with 300 µl DMSO (Fisher Scientific, Loughborough, UK) per well and the plate was left on a benchtop orbital shaker at 150RPM for 5 minutes. 200 µl from each well was transferred to a 96 well plate and absorbance was measured using a plate reader (Flexstation 3, Molecular Devices. λ = 490 nm).

Western Blotting

Western blotting was carried out in accordance to methods previously described [21, 35, 36]. In short, cells were lysed in lysis buffer (50mM Tris, 150mM NaCl, 1% Triton-X, all obtained from Sigma) containing a mini EDTA free protease inhibitor tablet (in 10ml of lysis buffer – Roche Applied Science, Burgess Hill, UK). We used primary rabbit polyclonal antibodies for GFAP (DAKO), GLT-1 (provided by Prof. David Pow, RMIT University, 1:5000 (0.04 µg/ml)) and Glutamine Synthetase (Abcam - ab49873, 1µg/ml) as cytoskeletal, transport and metabolic indicators of ‘reactivity’. Monoclonal goat anti mouse GAPDH (clone 6C5, 1:10000 (0.1µg/ml) - per 10µG protein load; Life technologies) was used as a reference protein. Primary antibodies were incubated overnight at 4°C in TTBS (20mM Tris buffer (pH 7.5 - Sigma) containing 0.4% Tween-20

(Sigma) and 1% non-fat milk powder). PVDF membranes were washed in TTBS and incubated with goat anti rabbit/goat anti mouse secondary antibodies conjugated to horseradish peroxidase (HRP – 1:5000 - Sigma) at room temperature (22°C) for 1 hour. After washing, membranes were further incubated with ECL reagent (Clarity, Biorad, Hemel Hempstead, UK) for 2 minutes. The ECL reagent was prepared according to manufacturer's protocol. Membranes were imaged using the Chemidoc MP imaging system (Biorad) for chemiluminescence and analysed by the corresponding ImageLab software (Biorad). Images were exported from the software at a resolution of 300dpi into photoshop CS3 and used for representation.

qPCR – Reactive Markers

RNA was extracted using RNA Bee (AMS Biotechnology, Abingon, UK). All RNA samples were collected from cells growing in 6 well plates on poly-L-ornithine treated plastic or Alvetex scaffold (8 x 10^5 cells per well). RNA Bee was added to each well (1 ml) on ice for 5 minutes. RNA was extracted in accordance to the manufacturer's protocol. RNA concentrations were calculated using a NanoDrop 2000 spectrophotometer (Thermo Scientific, Warrington, UK). A high capacity cDNA kit (4368814 - Life Technologies) was used to transcribe 1 µg of RNA. To perform PCR, the cDNA reaction mixture was diluted 1:20 in Tris-EDTA buffer (Sigma) and 5µl of cDNA was combined with 2 µl of both the forward and reverse primers (2.5 µM stock, final concentration 100 nM) and 7µl SYBR green (#170-8880 - Biorad). Oligonucleotide sequences were designed using the Primer3 website [37] and ordered through Sigma. Mus musculus LCN2/Serpina3n and connexin 43 were amplified using PCR and the following sets of oligonucleotides: LCN2 (F) 5'- ATGGCCCTGAGTGTCATGTG-3' (bases 23-43) and (R) 5'- ATGGCCCTGAGTGTCATGTG-3' (bases 162-182 - fragment

size 139 base pairs) based on first published sequence [38] (NCBI Accession number NM_008491.1).

Serpina3n (F) 5'- TGATGAGCATGGAGGACCTG -3' (bases 827-847) and (R) 5'-CTTCCACCTGCTGCATCTTG -3' (bases 964-984 - fragment size 138 base pairs) primers were designed based on original published sequences [39] (NCBI Accession number NM_009252.2). Connexin43 (F) 5'-GTCCCACGGAGAAAACCATC -3' (bases 837-857) and (R) 5'-GATCGCTTCTTCCCTTCACG-3' (bases 968-988 - fragment size 132 base pairs) primers were designed based on original published sequences [40] (NCBI Accession number NM_010288.3). GFAP (F) 5'-TTTCTCCAACCTCCAGATCC -3' (bases 1223-1243) and (R) 5'-GGTGAGCCTGTATTGGGACA -3' (bases 1335-1355 - fragment size 132 base pairs) primers were designed based on original published sequences [41] (NCBI Accession number NM_010277.3). Primer sequences for GLT-1 ((F) 5'-GCCAACAATATGCCCAAGCAG -3' (bases 10-30) and (R) 5'-GACACCAAACACAGTCAGTGA -3' (bases 153-133 - fragment size 144 base pairs)) were obtained from Primerbank (ID: 227330634c1) and ordered through Sigma. F+R denote forward and reverse primers. Primers were re-suspended in nuclease free water, to a concentration of 2.5μM. We used the Stepone Plus qPCR system (Applied Biosystems part of Life technologies) to assay changes in mRNA. CT values were exported from the software and comparative analysis was carried using relative quantification (RQ).

Statistical Analysis

Statistical comparison of treatment groups was carried out using unpaired students t-test unless otherwise stated (Prism 6, GraphPad Software, CA, USA).

Results

Astrocytes change shape when cultured in 3D scaffolds

Astrocytes were derived from NIH Swiss mouse embryos (E15) and postnatal (P4) mice. Embryonic cells were seeded directly onto coated glass coverslips or activated Alvetex and maintained for 12 days before experimental use. Postnatal cells were cultured in flasks for 18-21 days, trypsinised and re-plated onto coated glass coverslips or activated Alvetex scaffold. After 3 DIV, postnatal cells were either fixed or lysed for appropriate experiments. Astrocytes were characterized using epifluorescent microscopy, counterstaining for GFAP. Embryonic astrocytes have limited processes with small cell bodies close to each other in 2D (glass coverslip), (Fig 1,A). Postnatal astrocytes, have a more protoplasmic morphology in 2D (Fig 2, A). When cultured in Alvetex, the morphology changes for both embryonic and postnatal astrocytes, with astrocytes adopting a more protoplasmic phenotype (Fig 1, E; Fig 2, E).

Embryonic cells were plated at the same time and same density either into the scaffold or in 2D. We observed reduced mitochondrial succinate dehydrogenase activity (50% MTT turnover compared to 2D, data not shown) in the scaffold compared to 2D indicating reduced cell viability or cell number. Both embryonic-derived and postnatal-derived astrocytes grown in Alvetex have longer processes which stretch through the XZ plane (Fig 1H and Fig 2H), appear larger in size and are present throughout the scaffold. In 3D, cells show greater spreading which we attribute to the increased surface area of the Alvetex scaffold (Fig 1 E). Importantly, the scaffold can be imaged using Differential Interference Contrast (DIC) microscopy and cells can be visualized inside the scaffold (Fig 1, E+F and Fig 2 E+F).

Postnatal-derived astrocytes contain more microglia (not shown). Trypsinised postnatal astrocytes are much more robust, with many cells seeding into the scaffold (80% MTT turnover compared to 2D, data not shown).

Expression of astrocyte markers in embryonic cultures changes in 3D scaffolds

We next characterized the expression of a number of astrocyte markers, comparing 3D Alvetex cultures to the conventional 2 dimensional cultures, with both embryonic and postnatal-derived astrocytes.

For astrocytes derived from E15 embryos, the expression of some of the main astrocyte hallmarks was decreased in 3D in comparison to 2D cultures (Fig, 3). Using Western blotting, we compared 3D astrocytes to their 2D controls. Interestingly, we observed lower GFAP expression in 3D embryonic astrocytes compared to 2D controls (53 ± 8% reduction, $p < 0.05$, $n = 3$). Levels of GLT-1 were significantly lower in 3D embryonic astrocytes compared to 2D controls (36 ± 7% reduction, $p < 0.05$, $n = 3$). Furthermore, another glutamate transporter, glutamate-aspartate transporter (GLAST) was found at significantly reduced levels in 3D cultured astrocytes (64 ± 1% reduction, $p < 0.05$, $n = 3$). Levels of a key metabolic enzyme enriched in astrocytes, glutamine synthetase (GS), remained the same whether embryonic-derived cultures were grown in Alvetex or on glass coverslips.

Other markers of astrocytes were measured including the chondroitin sulphate proteoglycans (CSPGs) SMC3 [42] and NG2 [43] (Fig. 3). Both proteins were found in embryonic-derived astrocytes grown in 2D. In embryonic-derived astrocytes grown in 3D, SMC3 was undetectable and levels of NG2 were significantly lower than found in 2D cultures (70 ± 7% reduction, $p < 0.001$, $n = 3$).

Next we assayed mRNA levels to identify differences between 3D and 2D cultures from embryonic-derived astrocytes (Fig. 5A). Supporting the differences in protein levels, astrocytes in 3D cultures displayed reduced levels of GFAP (0.8 fold reduction ± 0.01, $p \leq 0.001$, $n = 3$) and GLT-1 (0.8 fold reduction ± 0.01, $p \leq 0.001$, $n = 3$) compared to 2D cultures. We also assayed some transcripts recently identified as being highly regulated during astrogliosis [13]. We chose LCN2 (lipocalin 2), serpina3n (serine (or cysteine) peptidase inhibitor, clade A, member 3N), PTX3 (pentraxin 3) and Cx43 (connexin 43). Embryonic cultures in 3D have lower mRNA levels compared to 2D controls for LCN2, Serpina3n, PTX3 and Cx43 (0.8 fold reduction ± 0.1 for all genes, $n = 3$)

Astrocyte markers in postnatal cultures show few differences when cultured in 3D scaffolds

In comparison to embryonic-derived astrocytes, astrocytes derived from postnatal CNS showed similar expression in both 2D and 3D cultures for nearly all proteins analyzed (Fig 4.). A key difference between postnatal-derived and embryonic-derived astrocytes is that there was negligible GLT-1 expression in postnatal-derived astrocyte cultures. The predominant glutamate transporter in postnatal astrocytes is GLAST and no difference was found between 3D and 2D cultures. In addition, the levels of GS, GFAP and NG2 were the same between postnatal astrocytes grown in 3D compared to 2D. The level of SMC3 was significantly lower in 3D cultures compared to 2D cultures (89 ± 6% decrease, $p < 0.001$, $n = 3$).

Using qPCR we assayed the expression profile of the reactive markers described above (Fig 5.). Postnatal-derived astrocytes grown in 3D displayed significantly increased levels of LCN2 (1.8 fold increase ± 0.3, $p < 0.05$, $n = 3$) and significant decreases in both PTX3 (0.5 fold reduction ± 0.1, $p < 0.05$, $n = 3$) and Cx43 (0.6 fold reduction ± 0.1, $p <$

0.01, n = 3). Levels of GFAP and GLT-1 did not change between 2D and 3D cultures. Levels of Serpina3n were increased in 3D (0.9 fold increase ± 0.3, n = 3), although this increase was not statistically significant (p = 0.0509).

Discussion

Astrocyte culture is a well-established technique necessary to understand the biology of these important cells and to provide an *in vitro* counterpart to in vivo models. Several groups have shown that culture of cells on 3D scaffolds can enhance astrocyte phenotype, indicative of a less 'reactive' expression profile [26, 30]. For first time we tested a commercially available material, Alvetex as a 3D scaffold. We chose this material because it is easy to prepare compared to collagen gels or fibers which require electrospinning, and Alvetex is reported to be physiologically inert. We sought to identify whether culturing in the scaffold alone could change the phenotype of astrocytes which had been derived from either embryonic or postnatal mice. To do this, we monitored the expression of the main astrocyte hallmarks finding differences for GLT-1, GFAP and GLAST in embryonic cultures along with CSPG markers of immature glia and some novel putative markers of reactive astrocytes. In summary, our results showed that astrocytes derived from embryonic tissues expressed markers of mature astrocytes when grown in either 2D or 3D, namely GFAP, GS and GLT-1. When grown in 3D, embryonic-derived astrocytes showed lower levels of expression than their 2D counterparts of GFAP and mRNA levels of a number of genes associated with reactive astrogliosis, namely LCN2, serpina3N, PTX3 and Cx43. In contrast, astrocytes derived from postnatal CNS expressed GFAP and GS but not GLT-1. Unlike primary astrocytes derived from embryonic tissue, these cultures, when grown in Alvetex did not show a profile associated with reduced reactivity, with some markers increasing and others

decreasing. Astrocytes derived from postnatal tissue importantly, lack a key transporter protein found in mature astrocytes, namely GLT-1.

One of the key findings is that in Alvetex, primary astrocytes derived from embryonic tissue displayed a morphology which is more similar to mature astrocytes in intact tissues than found in astrocytes grown on coverslips. Specifically, astrocytes grown on coverslips display a cobblestone like morphology, while in Alvetex the cells are smaller and have fine processes, supporting recent findings [29]. These differences in shape are accompanied by lower expression of GFAP. We associate a reduced GFAP with a less reactive phenotype: in vivo, astrocytes have low levels of GFAP unless there is CNS injury [15]. In addition to reduced GFAP, there are reduced levels of a number of transcripts encoding markers that have recently been associated with a reactive phenotype. Whilst these astrocytes are derived from embryonic tissue, they display a mature phenotype, including expression of GLT-1, an abundant protein in adult astrocytes and also low levels of the CSPGs NG2 and SMC3.

We have a particular interest in expression and regulation of the glutamate transporter, GLT-1 [27, 44] that is responsible for approximately 95% of all L-glutamate uptake in the CNS and accounts for about 1% of all CNS protein [5, 45, 46]. Recent transcriptomic data, confirms that GLT-1 is predominantly enriched in astrocytes [14, 45, 47]. It is known that GLT-1 expression is influenced by neuronal growth factors and the expression of GLT-1 declines in astrocytes during culture [48]. We have previously developed our embryonic-derived astrocyte culture in order to preserve expression of GLT-1, and the data confirms that these astrocytes support GLT-1 expression both in 2D and 3D culture. In contrast postnatal-derived astrocytes, which are re-plated and grown longer in culture (25 DIV in total, compared to 10-12 DIV for the embryonic-derived cultures), show negligible expression of GLT-1, though these cells maintain robust

expression of GLAST, a related transporter which accounts for less than 5% of all glutamate uptake in the mature CNS. These results support observations that cortical astroglial culture yields distinct populations of astrocytes depending on the method and age of the mice. Embryonic (E13-16) culture yields astrocytes rich in GLT-1, though confluent cells in 2D lose protoplasmic processes and have elevated levels of GFAP. In these cultures GLT-1 is lost over time in culture unless supplemented with G-5 supplement (EGF, FGF, Transferrin, Hydrocortisone, Selenite, Insulin, Biotin) which increases RNA and protein levels of both GLT-1 and GLAST [49]. Postnatal cortical astrocytes tend to grow as mixed glial cell populations, mainly astrocytes but with a higher proportion of microglia. Such cultures take longer to become confluent and whilst they too express high levels of GLAST; GLT-1 levels decrease over time, with the functional burden of glutamate transport assumed by GLAST [48, 50]. Indeed, research has shown that GLAST mediates the majority of L-glutamate uptake in postnatal cortical astrocyte cultures (28-35 *DIV*), correlating with increased cell surface expression of GLAST [22].

We also note that expression levels of GLT-1 were lower in embryonic-derived cultures grown in 3D compared to 2D. These results suggest the intriguing notion that reduced astrocyte reactivity is associated with lower levels of GLT-1. In disease or animal disease models, under conditions where astrocytes up-regulate GFAP there is often down-regulation of GLT-1 eg in Motor Neuron Disease [22, 30, 51]. Loss of GLT-1 during astrocyte reactivity is often associated with a loss of protective functions in astrocytes. Specifically, astrocyte GLT-1 loss has been linked to excitotoxic neuronal death in some disorders, particularly Motor Neuron Disease e.g [23-25, 52]. In this study we show that GLT-1 and GFAP expression appear to be co-regulated. The Alvetex

system provides an experimental platform to enable the study of astrocyte reactivity and co-regulation of GFAP and GLT-1.

In vitro, astrocytes have a high replicative capacity, another feature of gliosis. The latter stages of gliosis involve replication of immature reactive astrocytes and deposition of extracellular matrix proteins in an attempt to provide a physical barrier to any areas of insult in the brain [15, 46]. Rich in this region are CSPG's, a family of different core proteins that differ in their glycosaminoglycan motifs [52]. CSPG's fall into 4 main families with a range of functions in health and disease [53]. CSPG upregulation is a consequence of reactive astrogliosis and a feature of glial scarring. [54, 55]. We note that embryonic-derived astrocytes grown in 3D have low levels of the 2 CSPGs we measured, NG2 and SMC3, further support for these conditions supporting a less reactive, more physiologically representative phenotype. For postnatal-derived astrocytes, CSPGs were well expressed both in 2D and 3D cultures suggesting that these cultures have a more reactive phenotype that may be associated with their capacity for cell division.

We note recent evidence that the rho-kinase inhibitor Fasudil regulates astrocyte morphology through the re-distribution of actin, potentiating a neuroprotective astrocyte phenotype [56, 57]. Other work has shown that inhibition of the Rho-ROCK axis inhibits CSPG induced myosin phosphatase phosphorylation and reverses coffilin phosphorylation [58, 59] showing that CSPG and ROCK interaction regulate astrocyte morphology.

Differences between embryonic-derived and postnatal-derived astrocyte cultures are found in terms of morphology, GLT-1 and CSPG expression. Relative quantification of qPCR data revealed that postnatal cultures also have a different mRNA expression

profile in 2D and 3D compared to embryonic-derived cultures. Unlike embryonic-derived astrocytes, where all transcripts analyzed were lower in 3D culture compared to 2D culture, postnatal-derived astrocytes had higher LCN2 and serpina3n mRNAs in 3D compared to 2D, and unchanged GLT-1 and GFAP mRNA. Transcriptomic analysis of astrocytes obtained from two different injury models identified these genes as hallmarks of reactive astrocytes, particularly LCN2 which was upregulated greater than 200 fold in each model [13]. Interestingly, only LCN2 and serpina3n increase, whereas PTX3 and Cx43 remain very low.

As well as the protein and mRNA changes already discussed, there were differences in MTT turnover, indicating differences in cell viability or numbers in the Alvetex®, compared to cultures plated in 2D, even though cells were plated at the same densities. We believe this is due to non-adherence of cells to the scaffold, rather than toxicity. Alternatively the scaffold may inhibit cell division. Indeed, astrocyte culture with a 3D collagen scaffold has also shown a reduction in cell viability [26]. In this set of experiments, we did not look at the levels of NOTCH expression which may determine differences in proliferation in astrocytes [60, 61]. Further work will clarify these points in more detail. The differences in gene expression, protein expression and shape that we observe could potentially be attributed to culture confluency. We tested seeding at different densities onto Alvetex and did not observe any phenotypic or expression differences which related to cell viability as shown in Figure 3 (GFAP & GAPDH lanes) and data not shown, and attribute the differences we observe to the scaffold rather than the cell density. Further investigation would required to compare 3D and 2D cultures at the same cell densities, and we note that that this is difficult to control for, since the scaffold itself complicates quantifying cell numbers.

In conclusion in this study we show for the first time that Alvetex scaffolds are a suitable support for primary astrocyte cultures. We show that astrocytes display a less reactive phenotype than found on standard coverslips as evaluated by morphology and a range of biochemical markers. Furthermore we demonstrate that astrocytes derived from embryonic cerebral cortex have more of the phenotypic properties of mature, non-reactive astrocytes than astrocytes derived from postnatal brain that are passaged. Altogether this work suggests some technical advances to standardization and use of astrocyte cultures to understand astrogliosis and astrocyte function.

Acknowledgements

This manuscript would not be complete without mentioning Phil Beart, who has been an inspiration to the neurochemistry community for many years. Phil has sufficient citations already in his outstanding career for us to not feel the need to add to them substantially in this article. We acknowledge his positive influence on all aspects of this work and many of our other projects. As a proponent of astrocytes, glutamate transporters and – more recently – scaffolds, and with his love of the frosty tube we have enjoyed his generous company immensely over the years, and we wish him well. This work is supported through a BBSRC Industrial CASE PhD studentship, part funded by Pfizer, supporting CIU. WDH is an employee of Pfizer. The authors have no other commercial interests and no conflicts of interest to declare.

Figure Legends

Figure 1

Immunohistochemistry showing GFAP expression (green) in embryonic 2D (A-D) and 3D (E-H) cultures. Embryonic derived cells were seeded directly onto glass (2D) or Alvetex® (3D) scaffolds and maintained for 12 DIV (days in vitro). DIC microscopy permits visualisation of the Alvetex scaffold (E). 3 dimensional isosurface images of 2D (glass coverslip) (B+C) and 3D (Alvetex scaffold) (F+G) show number, shape and size of cells. XZ plots (D+H) show the Z plane. Embryonic-derived cells are found throughout the full width of the 3D scaffold. Nuclei are counterstained with Hoescht 33342 (blue). Scale bars = 10µm.

Figure 2

Immunohistochemistry showing GFAP expression (green) in postnatal-derived 2D (A-D) and 3D (E-H) cultures. Postnatal derived cells were trypsinised after 21 DIV (days in vitro), re-plated onto glass (2D) or Alvetex® (3D) scaffolds and maintained for a further 3 DIV. 3D isosurface images rendered in 2D (glass coverslip) (B+C) and 3D (Alvetex) (F+G) show number, shape and size of cells. XZ plots (D+H) show the Z plane, note that cells are found throughout the full width of the 3D scaffold. Nuclei are counterstained with Hoescht 33342 (blue). Scale bars = 10µm.

Figure 3

Western blotting was carried out for a number of protein markers of astrocytes using protein samples from embryonic-derived cultures (12 *DIV*). Panel (A) shows glutamate transporter (GLT-1: trimer 160 kDa and monomer 65 kDa), glutamine synthetase (GS, 45KDa). Lower blot shows glial fibrillary acidic protein (GFAP, 50 kDa). * indicates samples derived from cells plated at double the density. Glyceraldehyde Phosphate Dehydrogenase (GAPDH) was used as a sample loading control. Panel (B) shows glutamate transporter (GLAST: timer 160KDa, monomer 55 kDa) and the CSPGs SMC3

(140 KDa) and NG2 (250kDa). Panel (C) shows quantification of Western signals, first normalised to GAPDH, with the 3D levels expressed as a % of the 2D levels derived from parallel cultures. GLT-1, GFAP, GLAST, NG2 but not GS are found at reduced levels, with SMC3 levels too low to be quantified. Statistical analysis was carried out using student's t –test (* = $p<0.05$, **= $p<0.01$, ***=$p<0.001$). N = 3 independent cultures

Figure 4

Western blotting was carried out for a number of protein markers of astrocytes using protein samples from postnatal-derived cultures (25 *DIV*). Panel (A) shows glutamate transporter (GLAST: trimer 160 kDa and monomer 55 kDa), the CSPGs SMC3 (140 KDa) and NG2 (250kDa), glutamine synthetase (GS, 45KDa) and glial fibrillary acidic protein (GFAP, 50kDa). Glyceraldehyde Phosphate Dehydrogenase (GAPDH) was used as a sample loading control. Panel (B) shows glutamate transporter (GLT-1: trimer 160 kDa and monomer 65 kDa), which was barely detectable in most samples. Panel (C) shows quantification of Western signals, first normalised to GAPDH, with the 3D levels expressed as a % of the 2D levels derived from parallel cultures. SMC3 but not NG2, GLAST or GS are found at reduced levels(***=$p<0.001$, students t-test). N = 3 independent cultures

Figure 5

qPCR reveals differences in transcript levels of reactive markers in embryonic and postnatal 3D cultures when compared to their representative 2D controls. Graphs show RQ values represented as fold mRNA change on the y axis. Error bars represent SEM (n =3). GAPDH was used as a reference gene during relative quantification of CT values. (A) Embryonic-derived cultures have lower levels of LCN2, Serpina3N, GFAP, GLT-1, PTX3 and Cx43 measured when cultured in the 3D scaffold (*** = $p<0.001$,

Student's T test). B) For postnatal-derived cultures, LCN2 shows a significant increase in 3D whereas PTX3 and Cx43 show significant decreases in 3D scaffolds. GLT-1 and GFAP transcripts remain unchanged (* = $p<0.05$, ** = $p<0.01$, Student's T test).

References

1. Volterra A, Meldolesi J (2005) Astrocytes, from brain glue to communication elements: the revolution continues. Nature Reviews Neuroscience 6:626-640

2. Figley CR, Stroman PW (2011) The role(s) of astrocytes and astrocyte activity in neurometabolism, neurovascular coupling, and the production of functional neuroimaging signals. European Journal of Neuroscience 33:577-588

3. Sofroniew M, Vinters H (2010) Astrocytes: biology and pathology. Acta neuropathologica 119:7-35

4. Belanger M, Allaman I, Magistretti PJ (2011) Brain energy metabolism: focus on astrocyte-neuron metabolic cooperation. Cell Metabolism 14:724-738

5. Danbolt NC (2001) Glutamate uptake. Progress in neurobiology 65:1-105

6. Waagepetersen HS, Sonnewald U, Schousboe A (2003) Compartmentation of glutamine, glutamate, and GABA metabolism in neurons and astrocytes: functional implications. The Neuroscientist 9:398-403

7. Beart PM, O'Shea RD (2007) Transporters for L-glutamate: an update on their molecular pharmacology and pathological involvement. British Journal of Pharmacology 150:5-17

8. Johnson JA, Johnson DA, Kraft AD, Calkins MJ, Jakel RJ, Vargas MR, Chen PC (2008) The Nrf2-ARE pathway an indicator and modulator of oxidative stress in neurodegeneration. In: Gibson GE, Ratan RR, Beal MF (eds) Mitochondria and Oxidative Stress in Neurodegenerative Disorders. Blackwell Publishing, Oxford, pp 61-69

9. Halassa MM, Fellin T, Haydon PG (2007) The tripartite synapse: roles for gliotransmission in health and disease. Trends in Molecular Medicine 13:54-63

10. Araque A, Parpura V, Sanzgiri RP, Haydon PG (1999) Tripartite synapses: glia, the unacknowledged partner. Trends in Neurosciences 22:208-215

11. Bendotti C, Tortarolo M, Suchak SK, Calvaresi N, Carvelli L, Bastone A, Rizzi M, Rattray M, Mennini T (2001) Transgenic SOD1 G93A mice develop reduced GLT-1 in spinal cord without alterations in cerebrospinal fluid glutamate levels. Journal of Neurochemistry 79:737-746

12. Jeffery AF, Churchward MA, Mushahwar VK, Todd KG, Elias AL (2014) Hyaluronic acid-based 3D culture model for in vitro testing of electrode biocompatibility. Biomacromolecules 15:2157-2165

13. Zamanian JL, Xu L, Foo LC, Nouri N, Zhou L, Giffard RG, Barres BA (2012) Genomic analysis of reactive astrogliosis. The Journal of Neuroscience 32:6391-6410

14. Lovatt D, Sonnewald U, Waagepetersen HS, Schousboe A, He W, Lin JH, Han X, Takano T, Wang S, Sim FJ, Goldman SA, Nedergaard M (2007) The transcriptome and metabolic gene signature of protoplasmic astrocytes in the adult murine cortex. The Journal of Neuroscience 27:12255-12266

15. Sofroniew MV (2009) Molecular dissection of reactive astrogliosis and glial scar formation. Trends in Neurosciences 32:638-647

16. Sofroniew MV (2005) Reactive Astrocytes in Neural Repair and Protection. The Neuroscientist 11:400-407

17. Diaz-Amarilla P, Olivera-Bravo S, Trias E, Cragnolini A, Martinez-Palma L, Cassina P, Beckman J, Barbeito L (2011) Phenotypically aberrant astrocytes that promote motoneuron damage in a model of inherited amyotrophic lateral sclerosis. Proceedings of the National Academy of Science (USA) 108:18126-18131

18. Steele ML, Robinson SR (2012) Reactive astrocytes give neurons less support: implications for Alzheimer's disease. Neurobiology of Aging 33:423 e421-413

19. Faulkner JR, Herrmann JE, Woo MJ, Tansey KE, Doan NB, Sofroniew MV (2004) Reactive Astrocytes Protect Tissue and Preserve Function after Spinal Cord Injury. The Journal of Neuroscience 24:2143-2155

20. Myer DJ, Gurkoff GG, Lee SM, Hovda DA, Sofroniew MV (2006) Essential protective roles of reactive astrocytes in traumatic brain injury. Brain 129:2761-2772

21. Tortarolo M, Crossthwaite AJ, Conforti L, Spencer JP, Williams RJ, Bendotti C, Rattray M (2004) Expression of SOD1 G93A or wild-type SOD1 in primary cultures of astrocytes down-regulates the glutamate transporter GLT-1: lack of involvement of oxidative stress. Journal of Neurochemistry 88:481-493

22. Duan S, Anderson CM, Stein BA, Swanson RA (1999) Glutamate induces rapid upregulation of astrocyte glutamate transport and cell-surface expression of GLAST. The Journal of Neuroscience 19:10193-10200

23. Lange SC, Bak LK, Waagepetersen HS, Schousboe A, Norenberg MD (2012) Primary cultures of astrocytes: their value in understanding astrocytes in health and disease. Neurochemical Research 37:2569-2588

24. Kimelberg HK, Cai Z, Schools G, Zhou M (2000) Acutely isolated astrocytes as models to probe astrocyte functions. Neurochemistry International 36:359-367

25. Eng LF (1985) Glial fibrillary acidic protein (GFAP): the major protein of glial intermediate filaments in differentiated astrocytes. Journal of Neuroimmunology 8:203-214

26. East E, Golding JP, Phillips JB (2009) A versatile 3D culture model facilitates monitoring of astrocytes undergoing reactive gliosis. Journal of Tissue Engineering and Regenerative Medicine 3:634-646

27. Phillips JB (2014) Monitoring neuron and astrocyte interactions with a 3D cell culture system. Methods in Molecular Biology 1162:113-124

28. Puschmann TB, Zanden C, De Pablo Y, Kirchhoff F, Pekna M, Liu J, Pekny M (2013) Bioactive 3D cell culture system minimizes cellular stress and maintains the in vivo-like morphological complexity of astroglial cells. Glia 61:432-440

29. Hu WW, Wang Z, Zhang SS, Jiang L, Zhang J, Zhang X, Lei QF, Park HJ, Fang WJ, Chen Z (2014) Morphology and functions of astrocytes cultured on water-repellent fractal tripalmitin surfaces. Biomaterials 35:7386-7397

30. Lau CL, Kovacevic M, Tingleff TS, Forsythe JS, Cate HS, Merlo D, Cederfur C, Maclean FL, Parish CL, Horne MK, Nisbet DR, Beart PM (2014) 3D Electrospun scaffolds promote a cytotrophic phenotype of cultured primary astrocytes. Journal of Neurochemistry 130:215-226

31. O'Shea RD, Lau CL, Zulaziz N, Maclean FL, Nisbet DR, Horne MK, Beart PM (2015) Transcriptomic analysis and 3D bioengineering of astrocytes indicate ROCK inhibition produces cytotrophic astrogliosis. Frontiers in Neuroscience 9:50

32. Knight E, Murray B, Carnachan R, Przyborski S (2011) Alvetex(R): polystyrene scaffold technology for routine three dimensional cell culture. Methods in Molecular Biology 695:323-340

33. Juurlink BH, Hertz L (1985) Plasticity of astrocytes in primary cultures: an experimental tool and a reason for methodological caution. Developmental Neuroscience 7:263-277

34. Swanson RA, Seid LL (1998) Barbiturates impair astrocyte glutamate uptake. Glia 24:365-371

35. Ugbode CI, Hirst WD, Rattray M (2014) Neuronal influences are necessary to produce mitochondrial co-localization with glutamate transporters in astrocytes. Journal of Neurochemistry 130:668-677

36. Bahia PK, Pugh V, Hoyland K, Hensley V, Rattray M, Williams RJ (2012) Neuroprotective effects of phenolic antioxidant tBHQ associate with inhibition of FoxO3a nuclear translocation and activity. Journal of Neurochemistry 123:182-191

37. Untergasser A, Cutcutache I, Koressaar T, Ye J, Faircloth BC, Remm M, Rozen SG (2012) Primer3--new capabilities and interfaces. Nucleic Acids Research 40:e115

38. Hraba-Renevey S, Turler H, Kress M, Salomon C, Weil R (1989) SV40-induced expression of mouse gene 24p3 involves a post-transcriptional mechanism. Oncogene 4:601-608

39. Inglis JD, Lee M, Davidson DR, Hill RE (1991) Isolation of two cDNAs encoding novel alpha 1-antichymotrypsin-like proteins in a murine chondrocytic cell line. Gene 106:213-220

40. Yancey SB, Biswal S, Revel JP (1992) Spatial and temporal patterns of distribution of the gap junction protein connexin43 during mouse gastrulation and organogenesis. Development 114:203-212

41. Dyson PJ, de Smet C, Knight AM, Simon-Chazottes D, Guenet JL, Boon T (1992) Mapping of the genes encoding tum- transplantation antigens P91A, P35B, and P198. Immunogenetics 35:316-323

42. Chau CH, Shum DK, Li H, Pei J, Lui YY, Wirthlin L, Chan YS, Xu XM (2004) Chondroitinase ABC enhances axonal regrowth through Schwann cell-seeded guidance channels after spinal cord injury. The FASEB Journal 18:194-196

43. Dimou L, Gotz M (2014) Glial cells as progenitors and stem cells: new roles in the healthy and diseased brain. Physiological Reviews 94:709-737

44. Peacey E, Miller CC, Dunlop J, Rattray M (2009) The four major N- and C-terminal splice variants of the excitatory amino acid transporter GLT-1 form cell surface homomeric and heteromeric assemblies. Molecular Pharmacology 75:1062-1073

45. Cahoy JD, Emery B, Kaushal A, Foo LC, Zamanian JL, Christopherson KS, Xing Y, Lubischer JL, Krieg PA, Krupenko SA, Thompson WJ, Barres BA (2008) A transcriptome database for astrocytes, neurons, and oligodendrocytes: a new resource for understanding brain development and function. The Journal of Neuroscience 28:264-278

46. Giaume C, Kirchhoff F, Matute C, Reichenbach A, Verkhratsky A (2007) Glia: the fulcrum of brain diseases. Cell Death and Differentiation 14:1324-1335

47. Zhang Y, Chen K, Sloan SA, Bennett ML, Scholze AR, O'Keeffe S, Phatnani HP, Guarnieri P, Caneda C, Ruderisch N, Deng S, Liddelow SA, Zhang C, Daneman R, Maniatis T, Barres BA, Wu JQ (2014) An RNA-Sequencing Transcriptome and Splicing

Database of Glia, Neurons, and Vascular Cells of the Cerebral Cortex. The Journal of Neuroscience 34:11929-11947

48. Gegelashvili G, Danbolt NC, Schousboe A (1997) Neuronal soluble factors differentially regulate the expression of the GLT1 and GLAST glutamate transporters in cultured astroglia. Journal of Neurochemistry 69:2612-2615

49. Vermeiren C, Najimi M, Maloteaux J-M, Hermans E (2005) Molecular and functional characterisation of glutamate transporters in rat cortical astrocytes exposed to a defined combination of growth factors during in vitro differentiation. Neurochemistry International 46:137-147

50. Gegelashvili G, Civenni G, Racagni G, Danbolt NC, Schousboe I, Schousboe A (1996) Glutamate receptor agonists up-regulate glutamate transporter GLAST in astrocytes. Neuroreport 8:261-265

51. Wilkin GP, Marriott DR, Cholewinski AJ (1990) Astrocyte heterogeneity. Trends in Neuroscience 13:43-46

52. Hartmann U, Maurer P (2001) Proteoglycans in the nervous system - the quest for functional roles in vivo. Matrix biology 20:23-35

53. Galtrey CM, Fawcett JW (2007) The role of chondroitin sulfate proteoglycans in regeneration and plasticity in the central nervous system. Brain Research Reviews 54:1-18

54. Matsui F, Oohira A (2004) Proteoglycans and injury of the central nervous system. Congenital Anomalies 44:181-188

55. Sharma K, Selzer ME, Li S (2012) Scar-mediated inhibition and CSPG receptors in the CNS. Experimental Neurology 237:370-378

56. Lau CL, O'Shea RD, Broberg BV, Bischof L, Beart PM (2011) The Rho kinase inhibitor Fasudil up-regulates astrocytic glutamate transport subsequent to actin remodelling in murine cultured astrocytes. British Journal of Pharmacology 163:533-545

57. Lau CL, Perreau VM, Chen MJ, Cate HS, Merlo D, Cheung NS, O'Shea RD, Beart PM (2012) Transcriptomic profiling of astrocytes treated with the Rho kinase inhibitor fasudil reveals cytoskeletal and pro-survival responses. Journal of Cellular Physiology 227:1199-1211

58. Gopalakrishnan SM, Teusch N, Imhof C, Bakker MH, Schurdak M, Burns DJ, Warrior U (2008) Role of Rho kinase pathway in chondroitin sulfate proteoglycan-mediated inhibition of neurite outgrowth in PC12 cells. Journal of Neuroscience Research 86:2214-2226

59. Monnier PP, Sierra A, Schwab JM, Henke-Fahle S, Mueller BK (2003) The Rho/ROCK pathway mediates neurite growth-inhibitory activity associated with the chondroitin sulfate proteoglycans of the CNS glial scar. Molecular and Cellular Neurosciences 22:319-330

60. Magnusson JP, Göritz C, Tatarishvili J, Dias DO, Smith EMK, Lindvall O, Kokaia Z, Frisén J (2014) A latent neurogenic program in astrocytes regulated by Notch signaling in the mouse. Science 346:237-241

61. Chenn A (2009) A Top-NOTCH way to make astrocytes. Developmental Cell 16:158-159

Figure 1

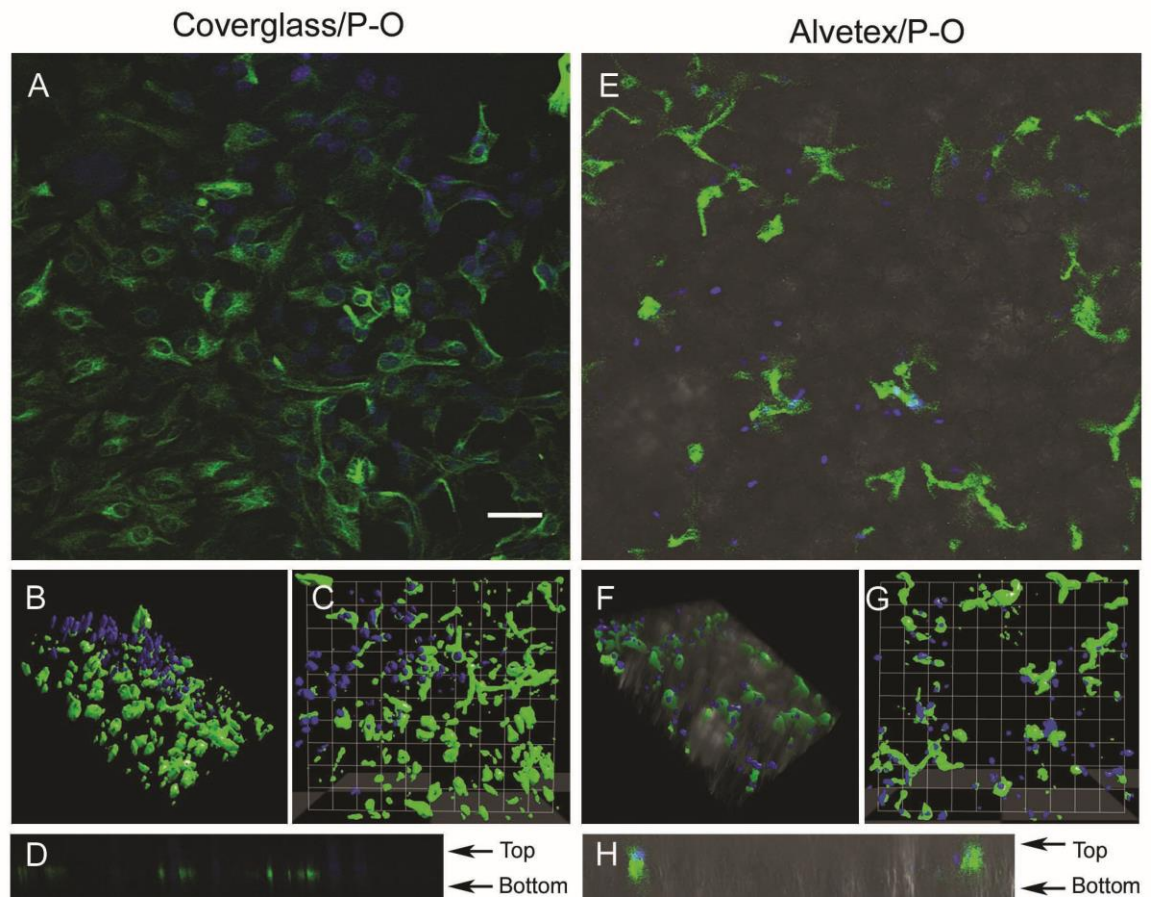

Figure 2

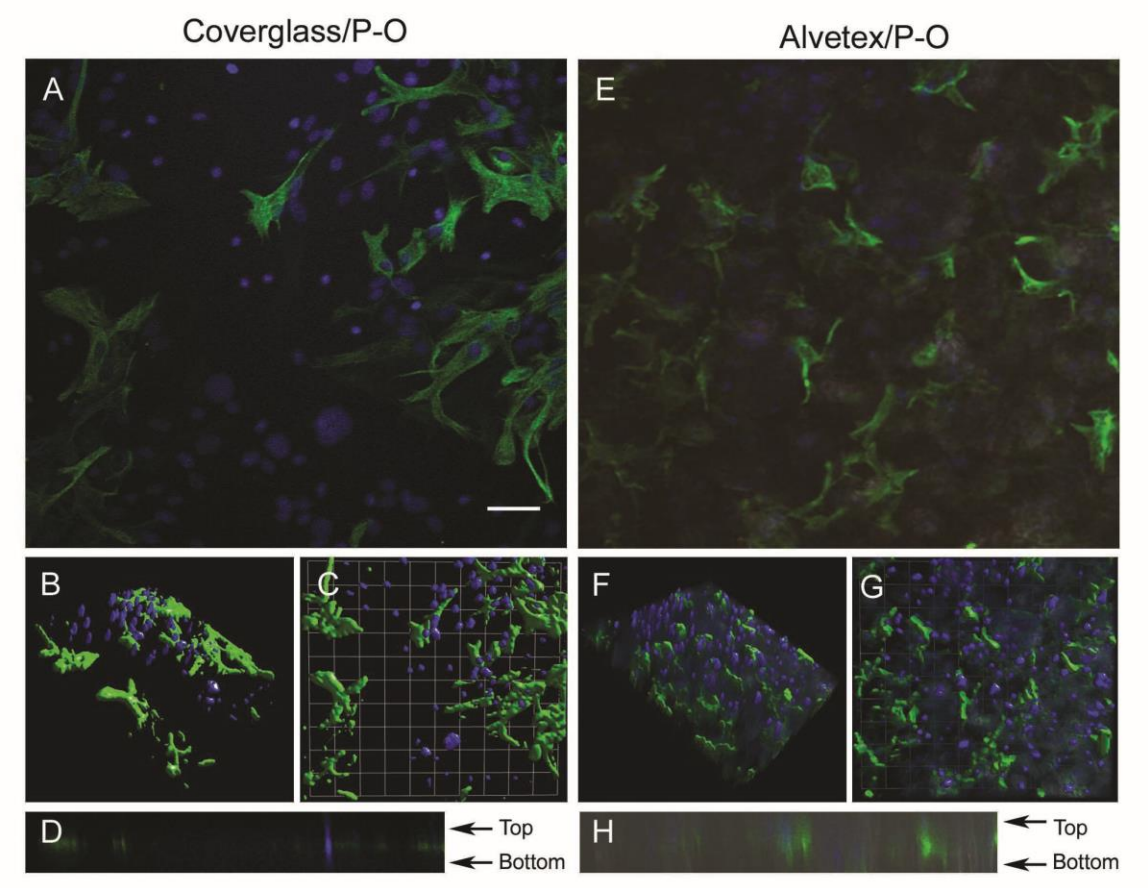

Figure 3

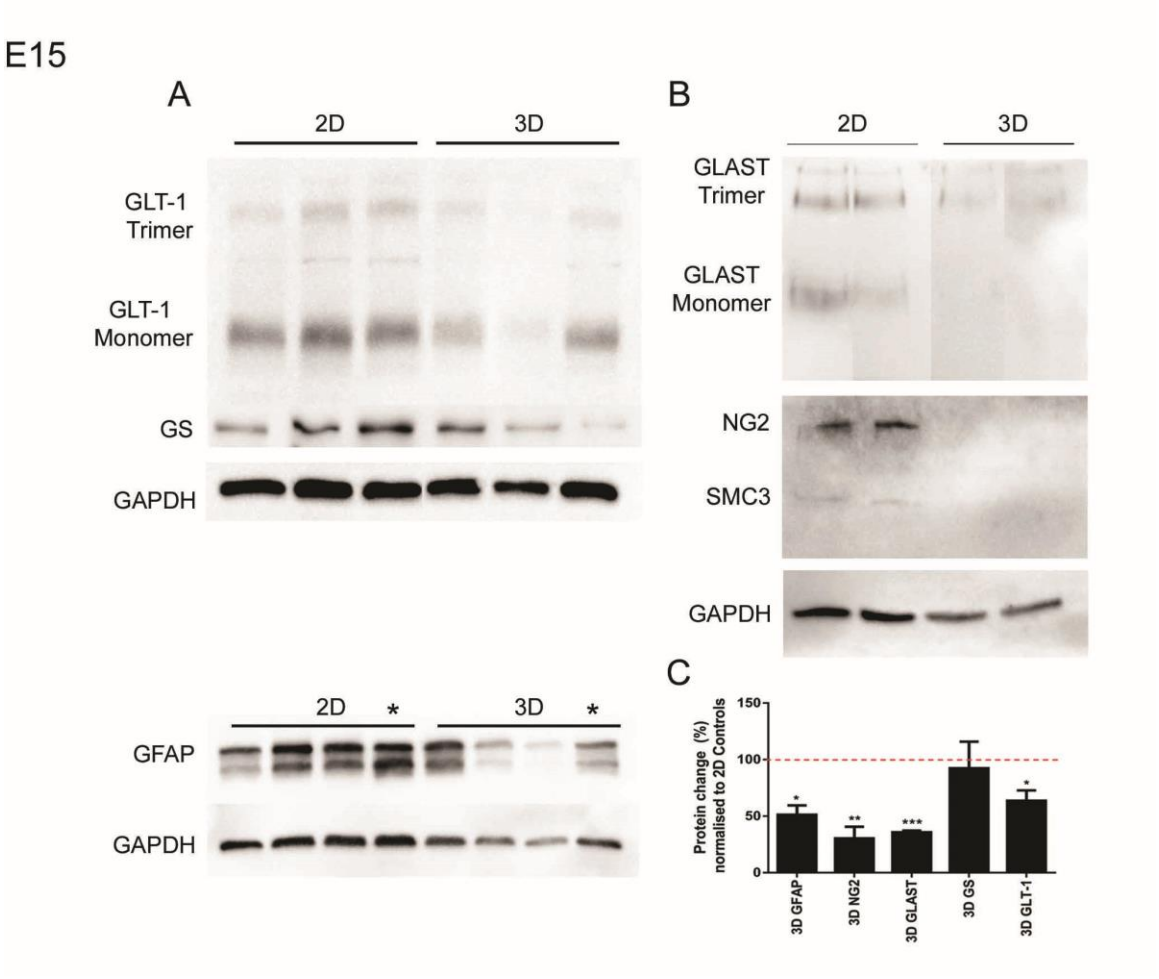
E15
A
2D
3D
GLT-1
Trimer
GLT-1
Monomer
GS
GAPDH
2D
*
3D
*
GFAP
GAPDH
B
2D
3D
GLAST
Trimer
GLAST
Monomer
NG2
SMC3
GAPDH
C
Protein change (%)
normalised to 2D Controls
150
100
50
0
*
**
***
*
3D GFAP
3D NG2
3D GLAST
3D GS
3D GLT-1

Figure 4

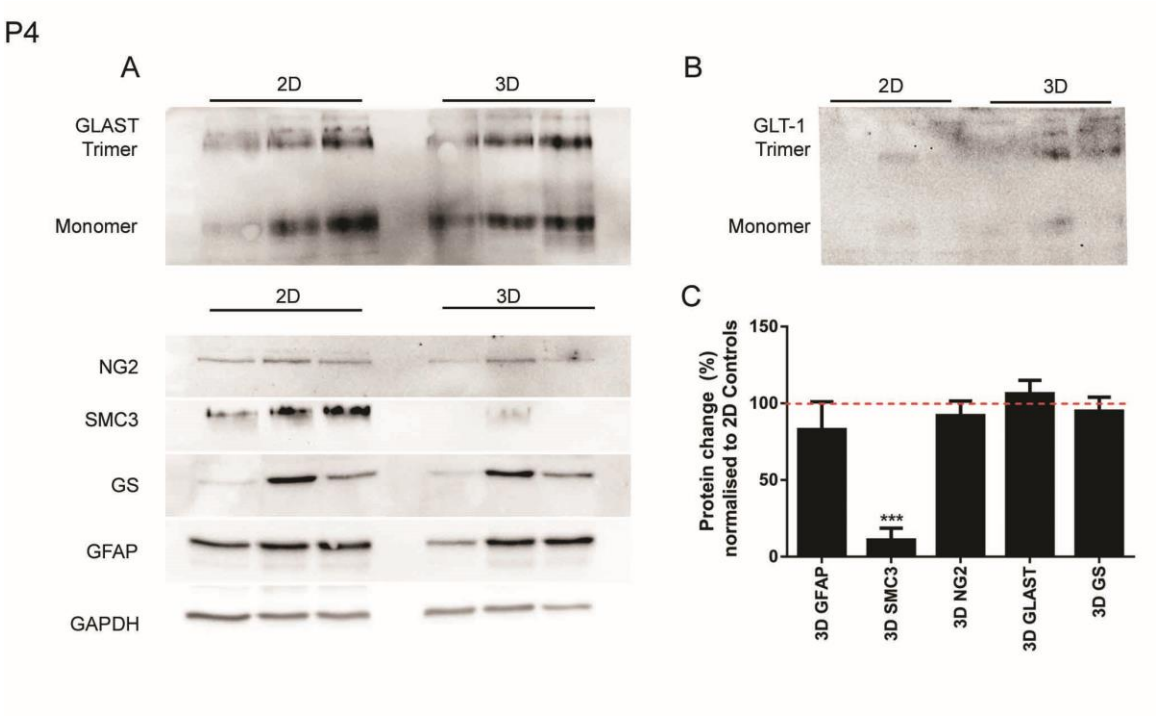
P4
A
2D
3D
GLAST
Trimer
Monomer
2D
3D
NG2
SMC3
GS
GFAP
GAPDH
B
2D
3D
GLT-1
Trimer
Monomer
C
Protein change (%)
normalised to 2D Controls
150
100
50
0
***
3D GFAP
3D SMC3
3D NG2
3D GLAST
3D GS

Figure 5

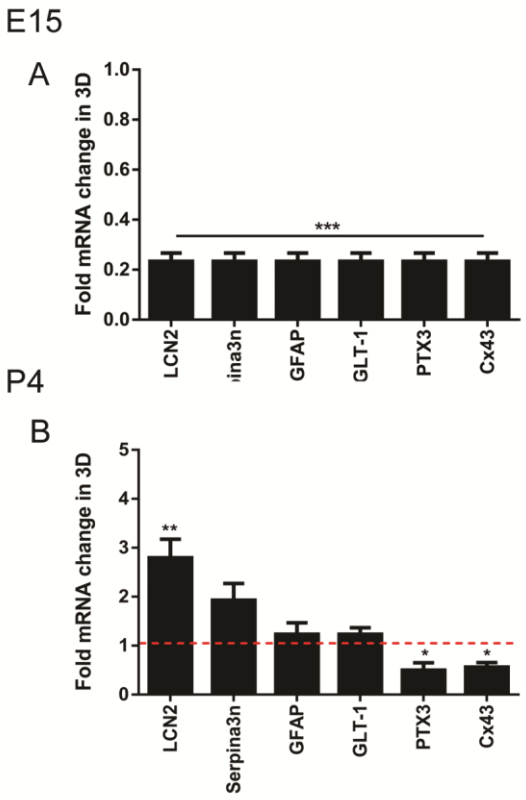
E15
A
Fold mRNA change in 3D
1.0
0.8
0.6
0.4
0.2
0.0
***
LCN2
ina3n
GFAP
GLT-1
PTX3
Cx43
P4
B
Fold mRNA change in 3D
5
4
3
2
1
0
**
*
*
LCN2
Serpina3n
GFAP
GLT-1
PTX3
Cx43